NIH Public Access
Author Manuscript
Int J Imaging Syst Technol. Author manuscript; available in PMC 2015 June 01.

Published in final edited form as:
Int J Imaging Syst Technol. 2014 June ; 24(2): 138–148. doi:10.1002/ima.22088.

NEUROFEEDBACK USING FUNCTIONAL SPECTROSCOPY

Oliver Hinds[1], **Paul Wighton**[2,3], **M. Dylan Tisdall**[2,3], **Aaron Hess**[4], **Hans Breiter**[5,6], and **André van der Kouwe**[2,3]

[1]Athinoula A. Martinos Imaging Center at the McGovern Institute for Brain Research, Massachusetts Institute of Technology

[2]Athinoula A. Martinos Imaging Center, Department of Radiology, Massachusetts General Hospital

[3]Harvard Medical School

[4]Department of Human Biology, MRC/UCT Medical Imaging Research Unit, University of Cape Town, South Africa

[5]Department of Psychiatry, Massachusetts General Hospital

[6]Department of Psychiatry and Behavioral Sciences, Northwestern University Feinberg School of Medicine

Abstract

Neurofeedback based on real-time measurement of the blood oxygenation level-dependent (BOLD) signal has potential for treatment of neurological disorders and behavioral enhancement. Commonly employed methods are based on functional magnetic resonance imaging (fMRI) sequences that sacrifice speed and accuracy for whole-brain coverage, which is unnecessary in most applications. We present multi-voxel functional spectroscopy (MVFS): a system for computing the BOLD signal from multiple volumes of interest (VOI) in real-time that improves speed and accuracy of neurofeedback. MVFS consists of a functional spectroscopy (FS) pulse sequence, a BOLD reconstruction component, a neural activation estimator, and a stimulus system. The FS pulse sequence is a single-voxel, magnetic resonance spectroscopy sequence without water suppression that has been extended to allow acquisition of a different VOI at each repetition and real-time subject head motion compensation. The BOLD reconstruction component determines the T2* decay rate, which is directly related to BOLD signal strength. The neural activation estimator discounts nuisance signals and scales the activation relative to the amount of ROI noise. Finally, the neurofeedback system presents neural activation-dependent stimuli to experimental subjects with an overall delay of less than 1s. Here we present the MVFS system, validation of certain components, examples of its usage in a practical application, and a direct comparison of FS and echo-planar imaging BOLD measurements. We conclude that in the context of realtime BOLD imaging, MVFS can provide superior accuracy and temporal resolution compared with standard fMRI methods.

The authors of this manuscript have no conflicts of interest to declare.

NIH-PA Author Manuscript
NIH-PA Author Manuscript
NIH-PA Author Manuscript

NIH-PA Author Manuscript

NIH-PA Author Manuscript

NIH-PA Author Manuscript

Keywords

Biofeedback; Spectroscopy; fMRI

1. INTRODUCTION

Moment to moment measurement of the blood oxygenation level-dependent (BOLD) signal allows manipulation of experimental stimuli based on the current brain state of the subject. Such manipulations can be used to train subjects to gain control of regional neural activation. For example, neurofeedback control experiments have shown that subjects can learn to regulate regional BOLD signal when trained using a neurofeedback stimulus, which provides access to BOLD signal levels updated in real-time (deCharms, 2008). Manipulations of BOLD estimates available in real-time can also be used to shape activation patterns (Bray et al., 2007) or to control behavioral performance (Hinds et al., 2009; Yoo et al., 2009) without providing neurofeedback. The ultimate goal of such experiments is to harness moment to moment changes in the BOLD signal to treat neurological disorders or to enhance normal function. Whether the goal of an experiment is self-regulation or behavioral control, rapid and accurate BOLD estimates from the brain region of interest (ROI) increase the likelihood of success (Rockstroh et al., 1990).

In this work we present a new method for measuring moment to moment changes in the BOLD signal called multivoxel functional spectroscopy (MVFS) that can improve the speed and accuracy of BOLD estimation compared with commonly employed methods for real-time fMRI. MVFS is a complete system for real-time BOLD estimation that includes four components: MR signal measurement, BOLD reconstruction, activation estimation, and experimental stimulus integration.

The MR signal measurement component of MVFS is a pulse sequence based on functional spectroscopy (FS; Hennig et al., 1994). With the exception of Kuo et al. (2011), all previous studies computing real-time BOLD signal changes have employed echo-planar imaging (EPI) or spiral imaging sequences, which are the dominant pulse sequences for functional magnetic resonance imaging (fMRI). Both EPI and spiral sequences are designed to acquire images from the entire brain in a short time, and therefore when applied to neurofeedback applications waste substantial time acquiring data from parts of the brain that are not needed to compute ROI BOLD signal estimates. Like Kuo et al. (2011), our motivation is to sacrifice (unused) spatial data for an increase in temporal resolution. MVFS uses an FS-based pulse sequence that only collects data from specific ROIs. This reduces acquisition time and avoids artifacts in EPI and spiral imaging that arise from the relatively long delay between excitation and readout.

In addition, the MVFS pulse sequence includes an optional per-measurement navigator-based prospective head motion correction mechanism. The MVFS pulse sequence is implemented in C++ using the IDEA platform to run on Siemens MR systems (Siemens Healthcare, Erlangen, Germany).

NIH-PA Author Manuscript

NIH-PA Author Manuscript

NIH-PA Author Manuscript

Once free induction decay (FID) data is measured from an ROI, data from all receive channels is combined using a singular value decomposition based method for noise reduction, resulting in a single FID signal. BOLD reconstruction is then employed to produce an estimate of the T2* decay time by fitting a single decaying exponential to the FID magnitude.

T2* estimates are used to estimate moment to moment neural activation via an incremental general linear model (GLM) fit. The model fit accounts for portions of the T2* estimates that arise from nuisance sources (such as subject head motion or low-frequency signal fluctuations) by including bases in the GLM design for each nuisance signal. The contribution of nuisance signals is removed by subtracting its reconstruction from the measured T2* signal, leaving just a portion due to neural activation changes and residual noise not accounted for in the model. The model also includes bases created using the experimental stimulus schedule to account for the neural response to experimental stimuli. Such a complete model fit allows incremental estimation of the signal baseline and residual variance, which can then be used to scale the neural portion of the T2* signal by the expected deviation due to noise, resulting in a neural activation estimate in units of standard deviation from baseline.

Once an activation estimate has been computed, it is used to modulate the stimulus presented to the subject in the MR scanner. For neurofeedback training experiments the activation estimate can be directly displayed to the subject, while in behavioral control experiments the stimulus is changed in an activation-dependent manner. MVFS provides a system that avoids substantial unnecessary delay between activation estimation and stimulus update.

We performed several tests of MVFS to evaluate its performance and to compare its neurofeedback estimates with those computed using standard methods. The data from these tests focused on three specific issues. The first issue was to use our implementation of MVFS to perform a direct comparison of BOLD activation sensitivity with that of EPI, a major technique used in prior studies computing real-time BOLD signal changes. The second issue was to validate our method for real-time coil combination by determining the error in coil combination weights relative to the amount of time spent collecting data to compute them. The third issue was to test the entire system of MVFS using a human subject performing a behavioral task and receiving real-time neurofeedback.

To test the first issue of benchmarking MVFS against EPI-based methods, we studied four healthy volunteers with MVFS of the visual cortex during visual stimulation using checkerboard patterns that reverse their contrast. Data from these subjects was also used to evaluate the second issue of validating our method of real-time coil combination. For this second issue, we simulated the real-time approximation to the singular value decomposition (SVD) combination method using the data from these four healthy volunteers and varying the number of measurements used to compute the estimates. Lastly, to test the overall viability of the MVFS system, we tested the integrated system on one healthy volunteer performing a repeated finger tapping task while viewing neurofeedback from that task.

NIH-PA Author Manuscript

NIH-PA Author Manuscript

NIH-PA Author Manuscript

2. METHODS

2.1 MR signal measurement

The MR pulse sequence used to measure the BOLD signal in MVFS is based on the FS sequence originally proposed by Hennig et al. (1994). This pulse sequence measures an FID from a rectilinear ROI at each repetition by first exciting the spins in a plane using a radio frequency (RF) pulse to tip the spins 90° while a slice selective magnetic field gradient is applied. This is followed by two successive inversion RF pulses, each with a slice selective gradient in a direction orthogonal to the first, timed to create two spin echos. The first RF pulse limits the magnetization to a slab, then the two refocusing pulses limit magnetization to a column (second pulse), then a rectilinear box (third pulse). In the MVFS pulse sequence, the bandwidth of the RF pulse is held constant, and the size of the ROI in each direction is controlled by the strength of the associated gradient. The location of the ROI is controlled by changing the center frequency of the RF pulse. Figure 1 shows a diagram of the FS sequence.

The FS pulse sequence is essentially a PRESS pulse sequence for single-voxel spectroscopy (Ordidge et al., 1985) but without water signal suppression. The result of a single FS measurement is therefore an FID where the overwhelming source of signal decay is T2* dephasing of the water protons within the ROI. Because the BOLD signal is exactly a measurement of the change in T2* (due to differences in the oxygenation content of blood and blood volume), FS is sensitive to changes in the BOLD signal, as demonstrated by Hennig et al. (1994).

FS BOLD measurements have potential advantages over more commonly employed whole brain fMRI sequences both in speed and accuracy. For spiral and EPI sequences--the dominant pulse sequences used for fMRI--a single slice can be acquired in an amount of time comparable to a single FS measurement, however usually many slices are collected to achieve coverage of a much larger portion of the brain, thus requiring a much longer total repetition time (TR). While a single slice EPI or spiral sequence could acquire data at the same rate as FS, this is rarely done in practice, and has not been reported in any published real-time fMRI study. Further, whole-brain imaging methods suffer from substantial spatial distortion in regions near interfaces between tissues with relatively large magnetic susceptibility inhomogeneity, which create nonuniformities in the main field that interfere with spin encoding. FS is more robust to such susceptibility inhomogeneities both because the main field shims can be tuned to uniformize just the field within the ROI, and because FS does not rely on phase encoding for spatial localization.

One potential drawback to current FS-based sequences, such as Kuo et al. (2011), is that no images are produced. This prevents real-time head motion correction, which is usually performed during real-time fMRI experiments (Weiskopf et al., 2007) using a prospective (Thesen et al., 2000) or real-time retrospective method (Cox and Jesmanowicz, 1999). We have addressed this issue by supplementing the MVFS pulse sequence with volume navigators (vNavs), which are a tool for real-time sample-based artifact correction. Previously, vNavs have been demonstrated for motion correction in structural and functional MR pulse sequences such as MPRAGE, T2SPACE and diffusion EPI (Tisdall et al., 2011;

NIH-PA Author Manuscript

NIH-PA Author Manuscript

NIH-PA Author Manuscript

Alhamud et al., 2012; Hess et al., 2011), as well as for motion correction and frequency and shim correction in spectroscopic imaging (Hess et al., 2010). Here, we use vNavs to correct head motion by embedding a very rapid, low-resolution, multi-shot, three dimensional EPI sequence between FS acquisitions, which provides images of sufficient quality to perform prospective motion correction (Thesen et al., 2000). After vNav acquisition, the translation and rotation of the head computed via prospective motion correction is used to adjust the center frequency of the RF pulses and/or the strength of the gradients for the next FS acquisition. This way the FS ROI tracks the motion of the subject's head.

Another potential drawback of the FS sequence as proposed by (Hennig et al., 1994) is that only a single ROI can be measured at once. This is especially problematic for real-time fMRI studies where it is advantageous to feedback an ROI BOLD estimate from which a second ROI signal has been subtracted to account for global BOLD signal changes due to respiration or scanner instrumentation-related signal drift. While others have addressed this by using gradients to encode a 1-dimensional column of voxels (Kuo et al., 2011), in this preliminary work we simply allow FS acquisitions from multiple ROIs on successive measurements. By manipulating the frequency of the RF pulses and the strength of the gradients, the position of the ROI can be changed arbitrarily between measurements.

The MVFS pulse sequence is currently implemented in Siemens IDEA pulse sequence programming environment. In addition to the parameters that are available for user modification in the Siemens single-voxel spectroscopy sequence, the user can specify the number of ROIs and the placement of each, as well as whether and when vNav motion correction should be used to correct for subject head motion. After acquisition, ROI FIDs are passed to the Siemens image reconstruction computer for BOLD signal reconstruction, which is described next.

2.2 BOLD reconstruction

The MVFS pulse sequence produces an FID timecourse per measurement for each receive coil element. The goal of BOLD reconstruction is to estimate the T2* decay time of the ROI signal from these FIDs. Our approach is to first combine the FIDs from each coil element into a single FID while taking advantage of the independent estimates of the FID from each coil to reduce noise, then to fit the resulting FID signal with a decaying exponential function to allow an estimate of T2*.

2.2.1 Coil FID combination—FID signals measured with different receive coils on the same measurement contain signal components of varying phase and magnitude due to differences in the position and orientation of the coil relative to the ROI. In the ideal, noise-free case, the coil-specific FIDs are identical up to a scaling factor equal to this coil sensitivity. In real-world measurements, all signals that disturb this relationship can be considered noise. We employ a method for combining FID signals across coils tailored to our case of uncorrelated, complex-valued Gaussian noise (Bydder et al., 2008).

The coil-combination method begins by constructing a matrix **F** that includes all the data collected over the entire scan. Rows of **F** represent all data collected at a particular sample, while columns represent all data collected with a single coil. If our scan was noise-free, **F**

NIH-PA Author Manuscript

NIH-PA Author Manuscript

NIH-PA Author Manuscript

would be rank 1, as it can be viewed as the outer product of the true FID signal within the ROI and the vector of coil sensitivities. In the case of uncorrelated, complex-valued Gaussian noise, the singular value decomposition (SVD) of **F** can be used to derive the maximum-likelihood estimate of the true FID and coil sensitivities. A detailed description of this method follows.

The FID signal $f_{c,t}$ represents FS data measured with coil *c*at measurement *t*. **F** is constructed by first concatenating $f_{c,t}$ by measurement into a single vector f_c that represents all the data samples collected with coil *c*, then stacking these vectors into **F** with dimensions total number of scan samples by number of coils. Row *n* of **F** represents the nth sample from each coil, while column *c* represents all data acquired with coil *c*. The SVD of **F** = **USV** is then used to remove unwanted signal components by identifying the singular vector in **U** that represents the ROI FID signal component and discarding all others. Splitting this singular vector u_s back into individual FIDs f_t, yields an FID signal for each measurement that has been denoised and combined across coils. In practice, the first singular vector can always be chosen as the ROI FID component u_1 because it is the dominant non-white noise portion of the signal.

This coil combination method requires all of the measured data to be available to compute the SVD, and thus is only applicable for offline computations. However, we can adapt this method for real-time use if we notice that the first right singular vector v_1 can be used as an alternate means of computing the combined FIDs up to a scaling because $u_1 \propto \mathbf{F} v_1$ In this framework v_1 can be viewed as a set of attenuation coefficients that specify the contribution of each coil to the combined signal. If v_1 is known *a priori*, we can compute a combined FID signal from any single measurement incrementally as $f_t = \mathbf{F}_t v_1$, where $\mathbf{F}_t$ is a matrix with columns made of the FIDs from each coil at measurement *t*. In practice we have found that estimation of the coil combine weights v_1 can be accomplished in a few measurements at the beginning of each scan (see Section 3.3).

2.2.2 FID fit for T2* decay—Once the combined FID f_t has been computed, the T2* decay time d_t of the FID can be estimated. FIDs collected without water suppression are well modeled as a single decaying exponential of the form

$$f_t[n] = a e^{\frac{-n}{d_t}},$$

where *n* indexes the sample in the FID, *a* is amplitude, d_t is signal magnitude decay time. To find d_t at each measurement, we determine the parameters of the exponential that minimize the squared error with the measured FID using a standard nonlinear minimum searching algorithm based on the simplex method proposed by Nelder and Mead (1965). Only the magnitude portion of the complex signal is used in the fit in order to speed convergence. In practice we have found that the phase is sufficiently linear in time that the magnitude-only fit allows a robust estimate of d_t. Figure 2 shows two example FIDs and T2* fits to data measured using FS under strong neural activation and during rest.

NIH-PA Author Manuscript

NIH-PA Author Manuscript

NIH-PA Author Manuscript

2.2.3 Reconstruction implementation—The BOLD reconstruction component of MVFS is implemented in C++ within the Siemens Image Calculation Environment (ICE) and runs on the image reconstruction computer of the scanner. Raw FID data from each coil is input to the reconstruction pipeline, which is fed to the MVFS BOLD reconstruction program. If the required number of measurements for computing v_1 have not yet been collected, the FID data are stored for later use. If the measurement represents the last required for computing v_1, all FID data are used to build **F**, which is then used to compute v_1 by computing an SVD using the Template Numerical Toolkit (http://math.nist.gov/tnt/overview.html) and JAMA/C++, a C++ implementation of the JAva MAtrix Library (http://math.nist.gov/javanumerics/jama/). After the coil weights v_1 are computed, the stored FID data can be coil combined for each measurement. For subsequent measurements, the FIDs across each coil are immediately combined into a single FID via a weighted average using the weights v_1.

As soon as f_t becomes available, d_t (the T2* decay time) is computed by fitting the exponential model using a C++ implementation (by John Bukardt) of Applied Statistics Algorithm 47 (O'Neill, 1971), which implements Nelder and Mead (1965). Once d_t is available, the BOLD reconstruction component opens a TCP/IP socket connection to an external computer that is running a custom designed server which listens for incoming T2* estimates.

2.3 Activation estimation

BOLD reconstruction makes a T2* estimate available for each measurement. The task of activation estimation is to discount non-neural signal sources affecting the measured T2* and to transform BOLD estimates into meaningful units. The MVFS activation estimation method is identical to that proposed by Hinds et al. (2010) for EPI-based activation estimation. For completeness, we will briefly review it in the context of MVFS.

The goal is to discard nuisance signals from each incoming T2* value d_t, while maintaining neural signal components. An estimate of the contribution of neural and nuisance signals to the timecourse $d_{1..t}$ is updated at each measurement by incrementally fitting a GLM (Gentleman, 1974; Cox et al., 1995)

$$d = N\gamma + X\beta,$$

where **N** is a design matrix made up of nuisance signal bases and **X** is a design matrix made up of neural signal bases, while γ and β weight the contribution of each basis to the timecourse. The design matrices and d grow in length by one row with each measurement (time-dependent subscripts have been omitted for clarity).

The incremental model fit yields estimates of γ and β which can be used to reconstruct the estimated signal contributions from each nuisance and neural basis at any measurement. Nuisance signals can then be removed from d_t by computing

$$\overset{\alpha}{d}_t = d_t - N_t\gamma,$$

NIH-PA Author Manuscript

NIH-PA Author Manuscript

NIH-PA Author Manuscript

Where N_t is the tth row of **N** and $\overset{\alpha}{d_t}$ is the signal portion due to estimated neural sources plus unmodeled noise.

The standard deviation of the residual mean squared error after the GLM fit

$$\sigma = \sqrt{\frac{\sum_{t=1..\tau}(N_t\gamma + X_t\beta - d_t)^2}{\tau - 1}}$$

provides an estimate of the expected deviation of any single measurement from the mean T2* signal due to unmodeled noise within the ROI. Computing σ provides a convenient way to convert activation signal into meaningful units (z-scores), as

$$z_t = \frac{\overset{\alpha}{d_t}}{\sigma}$$

In practice σ is computed with τ fixed to some number of initial measurements without experimental stimulus used estimate noise levels and to let the incremental fit converge (e.g., τ=30). Estimating σ using only the first τ scans ensures that the scale factor used to compute z_t is identical for all $t \geq \tau$, and thus ensures consistent units for neurofeedback over the entire scan. Conceptually, the *z*-score z_t is the number of standard deviations the activation signal is from the expected baseline activation at time *t*.

The MVFS activation estimation component runs on a computer external to the scanner system, which will be called the processing/stimulus computer. Implementations are available both in C++ and in MATLAB (Hinds et al., 2010), and both achieve rapid processing, taking only a few milliseconds to process a single measurement with modern computer hardware. A custom TCP/IP server runs on the processing/stimulus computer that accepts incoming connections from the BOLD reconstruction component and initiates transfer of d_t as soon as a new measurement has been processed.

2.4 Experimental stimulus integration

Experimental stimuli that are dependent on moment to moment activation estimates should introduce as little delay as possible between the time a new estimate is available and the time that the stimulus display is updated. We have developed a stimulus integration component of MVFS that allows construction of stimuli that rapidly incorporates moment to moment activation estimates. Stimulus presentation is accomplished with the Pyschophysics Toolbox (Brainard, 1997), which runs within MATLAB on Linux, Macintosh, or Windows operating systems. Templates are provided for frequently employed real-time BOLD stimulus types such as thermometer-based neurofeedback training and activation-contingent presentation for behavior control (Hinds et al., 2009; Yoo et al., 2009).

The most recently computed activation estimates are made available to the stimulus script via compiled Matlab EXecutable (MEX) libraries implemented in C++. The library receives and stores z_t from the estimation component, then the stimulus script can access the most

NIH-PA Author Manuscript

NIH-PA Author Manuscript

NIH-PA Author Manuscript

recent (or any arbitrary) z_t with a single function call. The activation estimation and stimulus code execute in different threads, so latency from executing computationally intensive stimulus tasks is minimized.

3 Demonstration

In this section we demonstrate that MVFS provides a feasible alternative to EPI for measuring the BOLD signal in real-time. We first present a direct comparison of BOLD signal measurements with both FS and a commonly employed real-time fMRI acquisition scheme based on EPI. Also, we describe how FS increases acquisition speed compared with standard EPI-based real-time fMRI and validate our real-time adaptation of the SVD-based method for coil combination. We end the section with a demonstration of the complete neurofeedback system with a human subject.

3.1 Direct comparison of the magnitude of FS and EPI for real-time fMRI

The MVFS pulse sequence implements interleaved EPI and FS acquisitions. The generality of the vNav system allows us to modify the TE of the EPI navigator to detect the BOLD signal. This allows the same BOLD signal to be measured with both sequences almost simultaneously. Here, we used interleaved FS and EPI acquisitions to measure the BOLD sensitivity of these two methods by comparing BOLD signal changes under strong neural activation in the visual cortex.

Four subjects underwent MR scans during visual stimulation with checkerboard patterns that reverse their contrast at 8Hz. Such stimulation is known to produce relatively strong blood oxygenation changes in visual cortex (Fox and Raichle, 1984). All MR runs began with 30s of initial fixation to estimate a baseline neural state. The initial baseline period was followed by visual stimulation in a block design consisting of 5 block pairs, each of which contained 16s of fixation and 16s of checkerboard stimulus. Each run ended with 16s of fixation to allow activation to return to baseline. All subjects provided informed consent in accordance with the policies of Massachusetts General Hospital.

All acquisitions were collected using a 1.5T Avanto Siemens MR system. The first run for each subject was used as a functional localizer scan to locate an ROI particularly active during visual stimulation. Whole-brain EPI volumes were collected during the functional localizer scan with parameters: TR=2s, bandwidth/pixel=2298Hz, TE=40ms, matrix size=64×64, voxel size=3×3mm^2, slice thickness=3. 6mm, 32 slices, and 106 measurements, the first 3 of which were discarded to allow a magnetization steady state to develop. PACE (Thesen et al., 2000) was applied to incoming volumes during acquisition to correct for scan to scan subject head motion.

Immediatly after acquisition, the data was analyzed to locate voxels responsive to the visual stimulus using the FSL fMRI analysis software package (http://www.fmrib.ox.ac.uk/fsl/). Volumes were smoothed with a three dimensional Gaussian kernel of full width at half maximum of 6mm^3, high-pass filtered (cutoff 32s), prewhitened to account for timeseries autocorrelation, and fit to a GLM containing bases made up of the block design stimulus

NIH-PA Author Manuscript

NIH-PA Author Manuscript

NIH-PA Author Manuscript

schedule convolved with a double gamma model of the hemodynamic response and its first temporal derivative. An example activation pattern from one subject is shown in Figure 3.

Visualization of the functional localizer activation pattern allowed identification of a center of particularly strong activation in each subject. The coordinates of this spot were recorded for use during subsequent scans as the target for both FS and EPI activation estimation. An FS ROI of size 9×9×9mm^3 was centered on the target location. For direct comparison, we wanted to measure BOLD from an EPI ROI covering the same cortex as the FS ROI. To accomplish this a single 9mm thick EPI slice was centered on the target location and oriented to match the angle of the FS ROI. Because the in-plane EPI voxel size was 3mm^2, the 3×3 grid of voxels from the center of the EPI slice target the exact same brain tissue as the FS ROI. The EPI parameters for these comparison scans were the same as for the functional localizer scan except for the number of slices (one) and the slice thickness (9mm). FS parameters were: TE=40ms, bandwidth=2300Hz, and vector size=1024. Both FS and EPI had a TR of 2s individually.

Three scans were performed for each subject to compare EPI and FS BOLD measurements. First a scan using either just FS or just EPI individually was performed, then a scan using the combined FS/EPI pulse sequence was performed, then another individual scan was performed using the other of the methods used in the first scan. The order of individual scans was balanced across subjects: two subjects had the FS scan first and two had the EPI scan first. Figure 4 shows the results of both the individual and simultaneous comparison scans. Qualitative inspection reveals that FS is more sensitive to BOLD signal changes than EPI in both the simultaneous and the individual comparison scans.

The mean stimulus response *z*-scores were used to test quantitatively whether the BOLD sensitivity of FS is greater than EPI. Each timecourse was fit using a GLM with bases to model the expected neural response pattern as well as low frequency drift signals. This fit yields a pair of model parameters (one for FS and one for EPI) for each subject that represent the mean *z*-score of the visual stimulus response over the scan. These parameters were entered into a one-tailed, paired *t*-test across subjects to determine whether FS has a greater BOLD sensitivity than EPI. These tests were performed independently for simultaneous and individual scans. FS was found to be significantly more sensitive to BOLD than EPI for the simultaneous acquisition scans (t_3=2. 4; p=0. 049), while no significant difference between the two methods was found for individual scans (t_3=1.22; p=0. 15).

3.2 Acquisition speed comparison

For MVFS, the ROI selection RF pulses and gradients take a time equal to the specified echo time for the measurement. With modern MR systems this time can be very small (<10ms), however in practice it is desirable to use an echo time that maximizes BOLD sensitivity. For main field strengths in common use, the best echo time for BOLD will be substantially longer than the minimum achievable: from ~40-50ms for 1.5T (Turner et al., 1993; Fera et al., 2004) down to ~23ms for 7T (Yacoub et al., 2001). This value will dictate a relatively unchangeable amount of time devoted to MVFS ROI selection, which will vary slightly with field strength.

NIH-PA Author Manuscript

NIH-PA Author Manuscript

NIH-PA Author Manuscript

The amount of time devoted to FID readout, on the other hand, can be modified depending on the desired temporal sampling. In all the examples of MVFS we present here, a bandwidth of 3000Hz and vector size (number of FID samples) of 1024 was used. In this scheme an FID readout takes 340ms, determining a minimum repetition time of 420ms (accounting for the constant 80ms required for spoiling at the end of the sequence) at 1.5T. This minimum can be reduced substantially by reducing the vector size or increasing the bandwidth. For example, using a bandwidth of 5000Hz and a vector size of 256 a repetition time of 130ms can be achieved with an echo time of 40ms. In practice the specifics of the application will determine the balance between the bandwidth, vector size, and repetition time, which respectively affect the SNR, the length of the measured FID, and the temporal resolution.

When using vNavs for online subject head motion correction there is an additional amount of time devoted to acquiring the low-resolution, whole brain EPI volume at each TR. On our Avanto system (and on 3T Siemens Trio systems) a navigator volume with 32 image slices and a 32×32 matrix size can be acquired in 275ms using the maximum bandwidth, minimum echo time, and 6/8 partial Fourier encoding. Therefore the minimum repetition time achievable with motion corrected MVFS is 405ms when using an echo time of 40ms. This vNav is sufficient to perform prospective motion correction to within an accuracy of approximately 0.5mm (Tisdall et al., 2011).

In EPI, the temporal resolution is mainly limited by the number of slices acquired. Each slice requires a fairly short amount of time, e.g. 57ms using our Siemens Avanto system with a 6464 matrix size, an echo time of 40ms, and bandwidth of 2298Hz. Therefore 7 EPI slices can be acquired in the same amount of time as a single MVFS ROI. While it is possible to compute neurofeedback using 7 EPI slices, the ability to perform motion correction would be compromised. Practically, a minimum of 10 (and usually 16 or more) EPI slices are acquired per measurement (Weiskopf et al., 2004; Caria et al., 2007; Bray et al., 2007), which dictates an effective TR of 570ms. Therefore, MVFS provides a substantial increase in temporal sampling of the BOLD response over EPI when motion correction is not applied, and even with motion correction, MVFS provides a speedup compared with real-time EPI acquisitions in common use.

Very rapid temporal sampling can be achieved with MVFS while still applying vNavs if motion correction is limited to specific times during the scan when neurofeedback need not be computed. For example, if a few repetitions are available between temporal blocks or trials of neurofeedback, vNavs can be acquired only in these intervening times. This scheme will account for low-frequency drifts in head position while maintaining a BOLD sampling rate on the order of 100ms. Our implementation of MVFS allows collection and application of vNavs at arbitrary times during the scan. The time required to reconstruct the T2* signal was substantially less than 100ms, therefore computation time of signal reconstructions was never a bottleneck even when motion correction was not applied.

3.3 Coil combination method validity

We measured the performance of the real-time approximation to the SVD-based coil combination method described in Section 2.2.1 for increasing numbers of included

NIH-PA Author Manuscript

NIH-PA Author Manuscript

NIH-PA Author Manuscript

measurements at the beginning of the scan. In the limit of including all measurements in the SVD, the coil combination weights are identical between the real-time approximation and the offline computation via direct SVD application. However, inclusion of all measurements is not feasible in practice because feedback data would not be available until after the scan was completed. Therefore, a balance must be achieved where coil combination weights are computed from a subset of the measurements at the potential cost of accuracy in the weight estimates.

To determine the error in the coil combination weights relative to the amount of time spent collecting data to compute them, we simulated the real-time approximation to the SVD combination method and varied the number of measurements used to compute the estimates. The FS data collected for the direct comparison with EPI was used for this purpose. We computed the coil combination weights that would be estimated using only the first *m* measurements and varied *m* from 10 to the number of measurements in the scan (106). The mean squared error between the coil combination weights computed using all the measurements in the scan and resulting coil combination weights $v^{1,m}$ for each *m* were computed.

Figure 5 shows the relative coil combination weight estimate error over number of included measurements averaged over all four subjects, with error bars in gray indicating standard error. There is a sharp drop off in coil combine error for increasing number of included measurements from 1 to about 10, at which point the error drops more slowly, but steadily, to zero when including the entire scan to compute coil combine weights. Interestingly however, the percent error is already only 0.013% when including only a single measurement in computing the coil weights. This suggests that the coil weights producing the best coil combination are very similar over consecutive measurements, validating our choice to use only a few measurements at the beginning of the scan to compute the weights. In addition, the low error observed when even using just one measurement to estimate combine weights suggests that in practice they can be estimated based on only the first measurement.

We also compared the SVD-based coil combination method to the widely used sum of squares (SoS) coil combination method (Bydder et al., 2002). SoS combination would not require combination weights to be estimated, and thus would simplify the coil combine process. However, as shown in Figure 6, the process of adding together the squares of very low magnitude signals results in substantial bias of the reconstructed FID. This known drawback of SoS combination in low SNR situations is especially prominent in the tail of the FID where signal is very low.

3.4 Demonstration of the complete neurofeedback system

We demonstrated the operation of the complete MVFS neurofeedback system using a human subject. The subject performed a task requiring repeated finger tapping while viewing a neurofeedback stimulus that displayed the current BOLD estimate. This demonstration was designed to illustrate the use of MVFS in a standard neurofeedback training experiment.

NIH-PA Author Manuscript

NIH-PA Author Manuscript

NIH-PA Author Manuscript

An initial functional localizer scan was performed to locate an ROI covering cortex involved in movements of the fingers. Standard, whole-brain EPI volumes were collected while the subject performed a finger tapping task in a block design (5 blocks, each of 16s of tapping and 10s of rest). Immediately after the scan ended, the volumes were transferred from the scanner computer to an external computer for fMRI analysis, which was accomplished using FSL in less than 5 minutes. A center of particularly strong finger tapping activation in the left motor cortex was chosen as the location of the MVFS ROI. Figure 7a shows the functional localizer activation and ROI location.

Once the ROI center was found, an MVFS scan was performed with neurofeedback while the subject performed the same finger tapping task used during the functional localizer. 30 measurements were collected and stored by the coil FID combination system to estimate the coil weights via the SVD-based scheme presented in Section 2.2.1. Once all 30 measurements were acquired, the SVD was computed, the coil combination weights were stored, and the combination was applied to the first 30 measurements, yielding an FID for each measurement. These FIDs were passed along to the BOLD reconstruction component. BOLD reconstruction to determine T2* always occurred as soon as an FID became available. This T2* estimate was then immediately sent to the processing/stimulus computer via ethernet connection.

When a T2* value was received by the processing/stimulus computer, it was incorporated into the incremental GLM fit. After 30 measurements (which come rapidly one after the other because the corresponding FIDs are sent just after the coil combination weights have been estimated), the standard deviation of the GLM residuals was computed and taken as the noise magnitude for that scan. The feedback stimulus then began its display by revealing a thermometer indicating the magnitude of the most recent BOLD change processed (see Figure 7c). The beginning of neurofeedback also triggered the commencement of the stimulus schedule. Figure 7b shows the neurofeedback values that were presented to the subject via the height of the thermometer over the course of the scan.

4 Discussion

We have developed, implemented and tested a complete system for neurofeedback called MVFS. This system has specific advantages in speed and accuracy compared to traditional EPI-based neurofeedback systems and introduces real-time head motion correction to spectroscopy-based neurofeedback systems (Kuo et al., 2011). Our hope is that MVFS will provide an alternative to EPI based systems in situations where its advantages can improve the quality of neurofeedback and therefore increase the success rate of neurofeedback experiments.

4.1 Advantages

4.1.1 BOLD sensitivity—We demonstrated that the FS pulse sequence has an equal or greater BOLD sensitivity compared to EPI. Reliable neurofeedback during self-regulation training experiments is crucial for subjects to develop control over regional activation. In Section 3.1 we showed that when FS and EPI measure the same BOLD response to neural activation FS has a higher sensitivity to activation induced changes than EPI. Despite a

NIH-PA Author Manuscript

NIH-PA Author Manuscript

NIH-PA Author Manuscript

substantially greater mean response amplitude under FS, no significant difference was found when BOLD was measured independently during dedicated runs. However, this may be due to the increased variance associated with measuring different BOLD timecourses with the two techniques.

Almost every component of MVFS provides a speed advantage over EPI. In common usage, the EPI pulse sequence acquires multiple slices, which greatly decreases the BOLD sampling rate within a given ROI. FS acquires an ROI BOLD measurement in a time comparable to that required to acquire a single slice in EPI, increasing BOLD sampling rate multiplicatively by the number of slices prescribed in a particular EPI protocol. A standard EPI scan (64×64×32) produces more than 2 orders of magnitude more raw data than a single FS scan (1024), which increases data transmission time and aspects of data processing such as coil combination.

One aspect of data processing that is faster with EPI is processing the raw data to obtain relative activation values (T2* for MVFS, image intensity for EPI). EPI uses a fast Fourier transform (FFT) for this purpose, which is substantially faster than the fitting of an exponential function using an iterative optimization technique that MVFS relies on. However, if speed in this aspect of data processing is important, the relatively expensive exponential model fit can be replaced with an FFT of the FID, followed by estimation of the line width of the water peak.

Additional speedups over EPI-based neurofeedback systems are realized by reducing the number of timeseries that need to be processed during the activation estimation component. MVFS needs to fit only a single ROI timecourse using the GLM described in Section 2.3, while standard EPI based methods would need to fit a GLM for each voxel in an ROI. In addition, after the model fit the resulting activation values need to be combined across the ROI in a way that faithfully represents the BOLD signal (Hinds et al., 2010).

4.1.2 Spatial Accuracy—Any method that measures T2* changes will be sensitive to magnetic field inhomogeneities induced by the difference in magnetic susceptibility between different substances within a sample. Such susceptibility inhomogeneity distortions are a common problem with EPI-based fMRI, and they interfere with the ability to measure BOLD changes within certain parts of the brain. MVFS can partially overcome this problem for small portions of the brain by using the dynamic shims to uniformize the magnetic field within the ROI only rather than attempting to make the field over the entire brain uniform.

4.1.3 Acoustic noise—EPI and spiral methods for fMRI cover large portions of *k*-space in a small amount of time, and therefore must rely heavily on rapid magnetic gradient changes. These gradient changes are accompanied by loud acoustic noise that can interfere with fMRI experiments where the acoustic environment is important either 1) by creating non stimulus-related neural activation or 2) by modifying an individual's perceptual state. Examples of studies using neurofeedback that could be affected by fMRI acoustic noise are studies where auditory activation is the target for neurofeedback training (Thompson et al., 2009) as well as vigilance, meditation, or sleep studies where measured brain state is used to

NIH-PA Author Manuscript

NIH-PA Author Manuscript

NIH-PA Author Manuscript

change experimental stimuli (Hinds et al., 2009). It should be noted, however, that the inclusion of vNavs for motion correction would increase the acoustic noise of MVFS.

4.2 Limitations

The advantages in speed and accuracy over EPI made possible with MVFS are not without associated disadvantages. Because FS produces no brain images it is much more difficult to perform quality assurance on data either during a scan or retrospectively. For example, it is common to retrospectively correct for subject head motion by spatially coregistering the EPI volumes that contain the BOLD measurements. This is not possible with MVFS as the BOLD measurements are only an FID from a single (or a few) ROIs.

We have provided partial compensation for this drawback in MVFS by allowing interleaved acquisition of EPI and FS. These EPI volumes can be acquired quickly compared with standard EPI for BOLD measurement because the resolution and contrast can be adjusted for adequate structural information and by ignoring BOLD contrast. This provides images for quality assurance and real-time motion correction, but retrospective motion correction is still not possible. This is not a major drawback for neurofeedback applications, as offline data processing is not possible.

With EPI-based neurofeedback, ROIs are made up of a set of voxels. Because an EPI ROI can be constructed from any voxels in the volume, EPI provides much more flexibility than MVFS in ROI shape. This feature is especially important when providing neurofeedback from a region with a shape that is not modeled well by a rectilinear region, or is a region with disconnected pieces. We feel that in practice a substantial portion of most brain regions can be modeled well by a single rectilinear region, and thus this limitation will not provide a serious drawback for MVFS in most cases.

Because EPI acquires an entire brain volume at each measurement, BOLD activation from several ROIs can be measured at once. In its current formulation MVFS is unable to estimate BOLD activation from more than one ROI at each measurement. This means that the effective TR of MVFS is the product of the single-voxel TR and the number of voxels to be measured. In practice it is fairly common to measure BOLD from multiple ROIs when computing neurofeedback to provide feedback that is a relative measure of the activation from two regions. In addition, subtraction of the BOLD signal present in an ROI separate from the target ROI can help to alleviate global BOLD nuisance signals like variability in respiration or heart rate. In practice this limitation is fairly minor considering that only a one or two additional ROIs would need to be measured with MVFS to allow nuisance signal discounting or multiple ROI feedback. This would increase the effective TR, but it would still be shorter than the TR for a standard fMRI scan.

Acknowledgments

This research was supported by NIH grants R33DA026104, R21MH096559, R01HD071664, P41RR014075, S10RR021110 and the Ellison Medical Foundation.

NIH-PA Author Manuscript

NIH-PA Author Manuscript

NIH-PA Author Manuscript

References

Alhamud A, Tisdall M, Hess A, Hasan K, Meintjes E, van der Kouwe A. Volumetric navigators for real-time motion correction in diffusion tensor imaging. Magnetic Resonance in Medicine. 2012

Brainard D. The psychophysics toolbox. Spatial vision. 1997; 10(4):433–436. [PubMed: 9176952]

Bray S, Shimojo S, O'Doherty J. Direct instrumental conditioning of neural activity using functional magnetic resonance imaging-derived reward feedback. Journal of Neuroscience. 2007; 27(28):7498. [PubMed: 17626211]

Bydder M, Hamilton G, Yokoo T, Sirlin C. Optimal phased-array combination for spectroscopy. Magnetic resonance imaging. 2008; 26(6):847–850. [PubMed: 18486392]

Bydder M, Larkman D, Hajnal J. Combination of signals from array coils using image based estimation of coil sensitivity profiles. Magnetic Resonance in Medicine. 2002; 47(3):539–548. [PubMed: 11870841]

Caria A, Veit R, Sitaram R, Lotze M, Weiskopf N, Grodd W, Birbaumer N. Regulation of anterior insular cortex activity using real-time fMRI. Neuroimage. 2007; 35(3):1238–1246. [PubMed: 17336094]

Cox R, Jesmanowicz A. Real-time 3D image registration for functional MRI. Magnetic Resonance in Medicine. 1999; 42(6):1014–1018. [PubMed: 10571921]

Cox R, Jesmanowicz A, Hyde J. Real-time functional magnetic resonance imaging. Magnetic Resonance in Medicine. 1995; 33(2):230–236. [PubMed: 7707914]

deCharms C. Applications of real-time fMRI. Nature Reviews Neuroscience. 2008; 9(9):720–729.

Fera F, Yongbi M, van Gelderen P, Frank J, Mattay V, Duyn J. EPI-BOLD fMRI of human motor cortex at 1.5 T and 3.0 T: sensitivity dependence on echo time and acquisition bandwidth. Journal of Magnetic Resonance Imaging. 2004; 19(1):19–26. [PubMed: 14696216]

Fox P, Raichle M. Stimulus rate dependence of regional cerebral blood flow in human striate cortex, demonstrated by positron emission tomography. Journal of Neurophysiology. 1984; 51(5):1109. [PubMed: 6610024]

Gentleman WM. Algorithm as 75: Basic procedures for large, sparse or weighted linear least problems. Applied Statistics. 1974; 23(3):448–454.

Hennig J, Ernst T, Speck O, Deuschl G, Feifel E. Detection of brain activation using oxygenation sensitive functional spectroscopy. Magnetic Resonance in Medicine. 1994; 31(1)

Hess A, Tisdall M, Andronesi O, Meintjes E, van der Kouwe A. Real-time motion and b0 corrected single voxel spectroscopy using volumetric navigators. Magnetic Resonance in Medicine. 2011; 66(2):314–323. [PubMed: 21381101]

Hinds O, Ghosh S, Thompson TW, Yoo JJ, Whitfield-Gabrieli S, Triantafyllou C, Gabrieli JD. Computing moment to moment bold activation for real-time neurofeedback. Neuroimage. 2010

Hinds O, Thompson TW, Gabrieli S, Triantafyllou C, Gabrieli J. Behavioral task enhancement by brain state monitoring using real-time fMRI [Abstract]. Soc Neurocience Abst. 2009 Sun 11:15AM, room N426.

Kuo A, Chiew M, Tam F, Cunningham C, Graham S. Multiecho coarse voxel acquisition for neurofeedback fmri. Magnetic Resonance in Medicine. 2011; 65(3):715–724. [PubMed: 21337404]

Nelder J, Mead R. A simplex method for function minimization. The computer journal. 1965; 7(4): 308.

O'Neill R. Algorithm AS 47: Function minimization using a simplex procedure. Applied Statistics. 1971; 20(3):338–345.

Ordidge RJ, Bendall MR, Gordon RE, Connelly A. Volume selection for in-vivo biological spectroscopy. Magnetic Resonance in Biology and Medicine. 1985:387.

Rockstroh B, Elbert T, Birbaumer N, Lutzenberger W. Biofeedback-produced hemispheric asymmetry of slow cortical potentials and its behavioural effects. International Journal of Psychophysiology. 1990; 9(2):151–65. [PubMed: 2228749]

NIH-PA Author Manuscript

NIH-PA Author Manuscript

NIH-PA Author Manuscript

Thesen S, Heid O, Mueller E, Schad L. Prospective acquisition correction for head motion with image-based tracking for real-time fMRI. Magnetic Resonance in Medicine. 2000; 44(3):457–465. [PubMed: 10975899]

Thompson TW, Hinds O, Ghosh S, Lala N, Triantafyllou C, Gabrieli S, Gabrieli J. Training selective auditory attention with real-time fmri feedback[Abstract]. Neuroimage. 2009 22 F-PM.

Tisdall M, Hess A, Reuter M, Meintjes E, Fischl B, van der Kouwe A. Volumetric navigators for prospective motion correction and selective reacquisition in neuroanatomical mri. Magnetic Resonance in Medicine. 2011

Turner R, Jezzard P, Wen H, Kwong K, Le Bihan D, Zeffiro T, Balaban R. Functional mapping of the human visual cortex at 4 and 1.5 Tesla using deoxygenation contrast EPI. Magnetic Resonance in Medicine. 1993; 29(2):277–279. [PubMed: 8429797]

Weiskopf N, Scharnowski F, Veit R, Goebel R, Birbaumer N, Mathiak K. Self-regulation of local brain activity using real-time functional magnetic resonance imaging (fMRI). Journal of Physiology-Paris. 2004; 98(4-6):357–373.

Weiskopf N, Sitaram R, Josephs O, Veit R, Scharnowski F, Goebel R, Birbaumer N, Deichmann R, Mathiak K. Real-time functional magnetic resonance imaging: methods and applications. Magnetic resonance imaging. 2007; 25(6):989–1003. [PubMed: 17451904]

Yacoub E, Shmuel A, Pfeuffer J, Van De Moortele P, Adriany G, Andersen P, Vaughan J, Merkle H, Ugurbil K, Hu X. Imaging brain function in humans at 7 Tesla. Magnetic Resonance in Medicine. 2001; 45(4):588–594. [PubMed: 11283986]

Yoo JJ, Hinds O, Thompson TW, Gabrieli S, Triantafyllou C, Gabrieli J. Enhancing memory acquisition using real-time fmri [Abstract]. Soc Neurocience Abst. 2009 Sun 10:45AM, room N426.

NIH-PA Author Manuscript

NIH-PA Author Manuscript

NIH-PA Author Manuscript

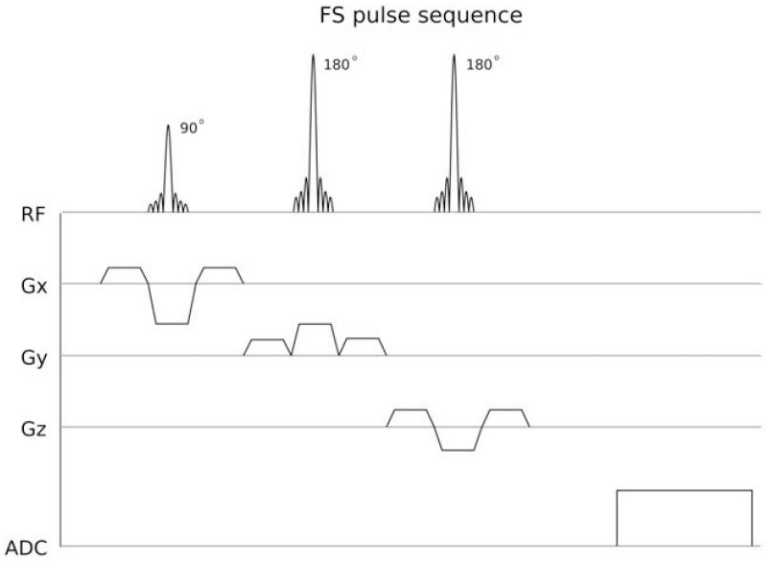

Figure 1.

FS pulse sequence diagram. The first 90° pulse excites a slab, the second pulse (180°) limits to a column, then the third pulse (180°) limits magnetization to a rectilinear box. The readout event measures the FID arising from the echo after the third pulse.

NIH-PA Author Manuscript

NIH-PA Author Manuscript

NIH-PA Author Manuscript

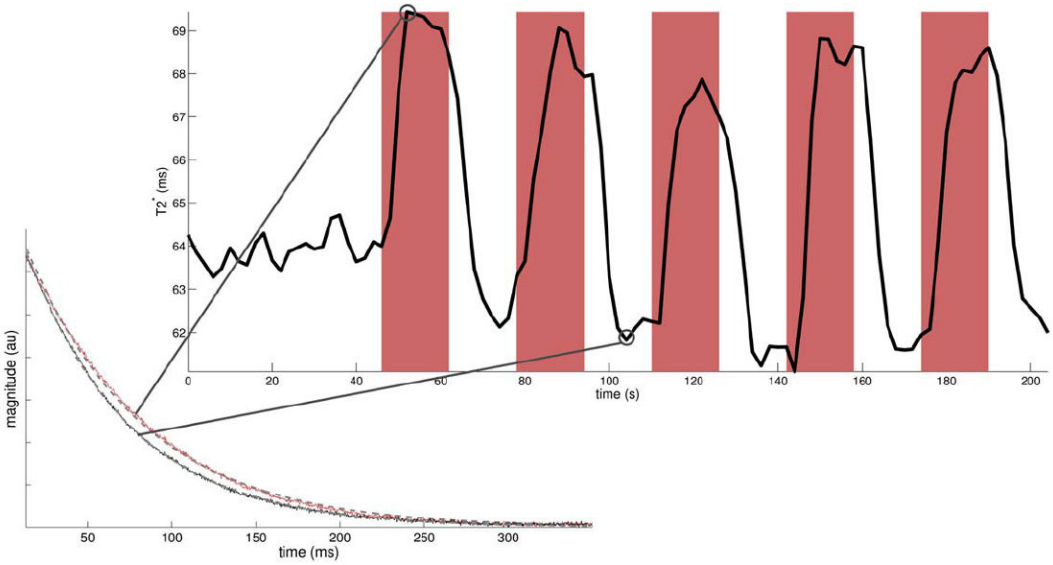

Figure 2.

Example FS FIDs during strong visual cortex stimulation (red) and passive fixation (black). The single fit to each is shown as a dashed gray line. The difference in T2* decay time due to visual stimulation is apparent by eye. The timecourse shows the change in T2* over an experimental run, with red regions indicating the presence of the visual stimulus. The excellent correlation with the stimulus time and the low noise level demonstrate the sensitivity of FS to neural activation as well as the stability of the T2* fit.

NIH-PA Author Manuscript

NIH-PA Author Manuscript

NIH-PA Author Manuscript

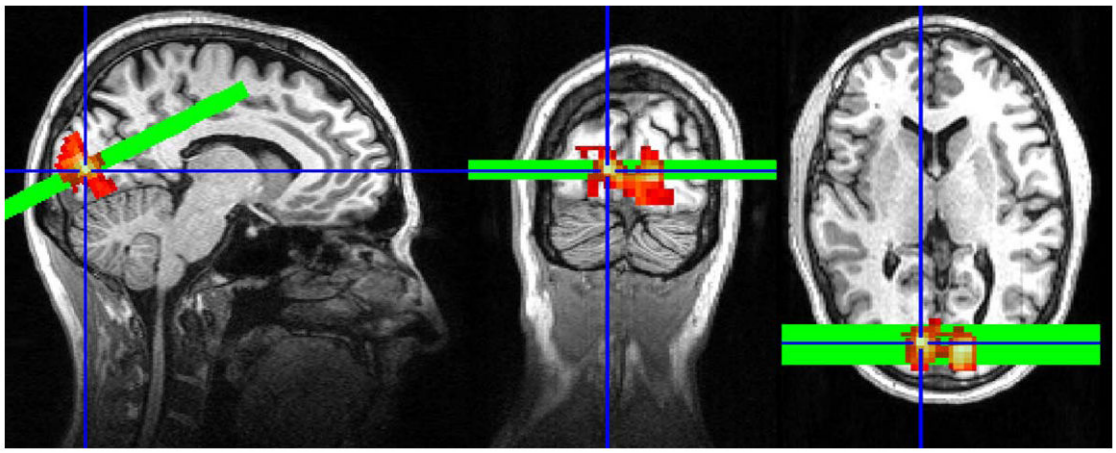

Figure 3.

Direct comparison of EPI and FS BOLD sensitivity for real-time fMRI. The heatmap shows the functional activation, from which the FS ROI was placed (blue crosshairs). The green plane indicates the location of the EPI slice.

NIH-PA Author Manuscript

NIH-PA Author Manuscript

NIH-PA Author Manuscript

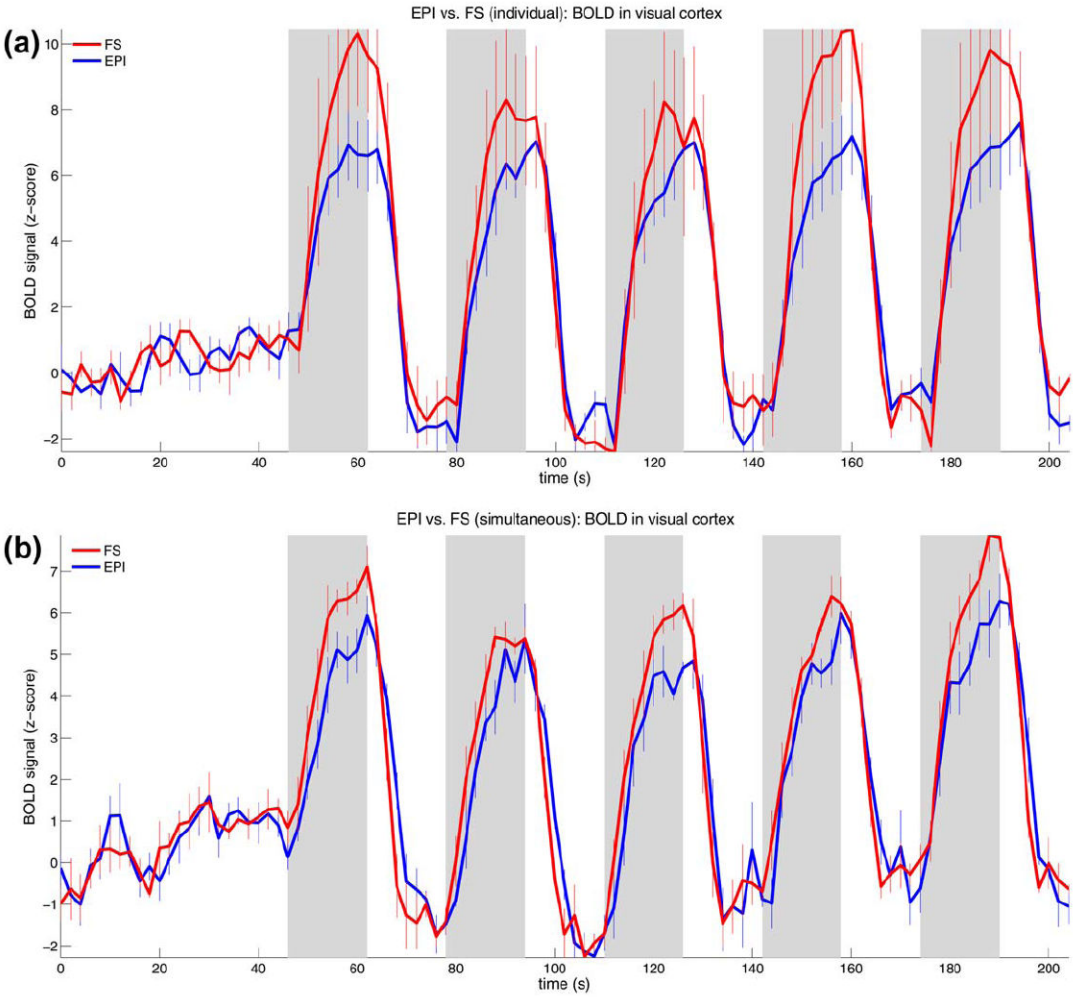

Figure 4.

Comparison of BOLD signal measured in visual cortex using FS and EPI. The top panel shows the BOLD signal across subjects during the individual sequence runs (FS and EPI were performed in separate runs). The bottom panel compares FS and EPI when used to sample the same BOLD signal simultaneously. In both cases FS has a higher BOLD sensitivity, but this difference is only significant for the simultaneous acquisition. [Color figure can be viewed in the online issue, which is available at wileyonlinelibrary.com.]

NIH-PA Author Manuscript

NIH-PA Author Manuscript

NIH-PA Author Manuscript

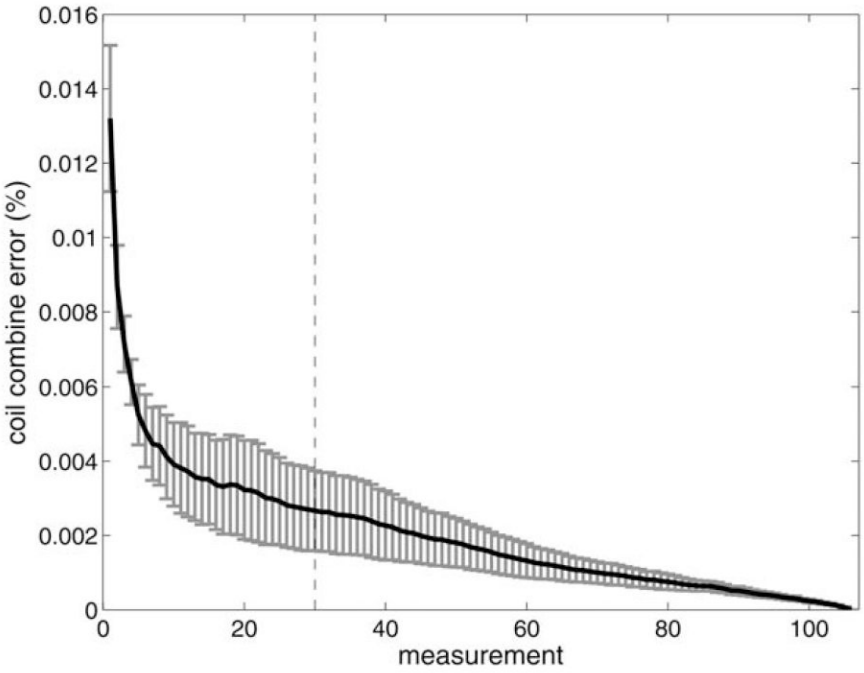

Figure 5.

The error in coil weighting factors when estimated from an increasing number of measurements from beginning of a scan compared to estimation from the full scan. In practice we use the value 30, which is indicated here by the vertical dashed line.

NIH-PA Author Manuscript

NIH-PA Author Manuscript

NIH-PA Author Manuscript

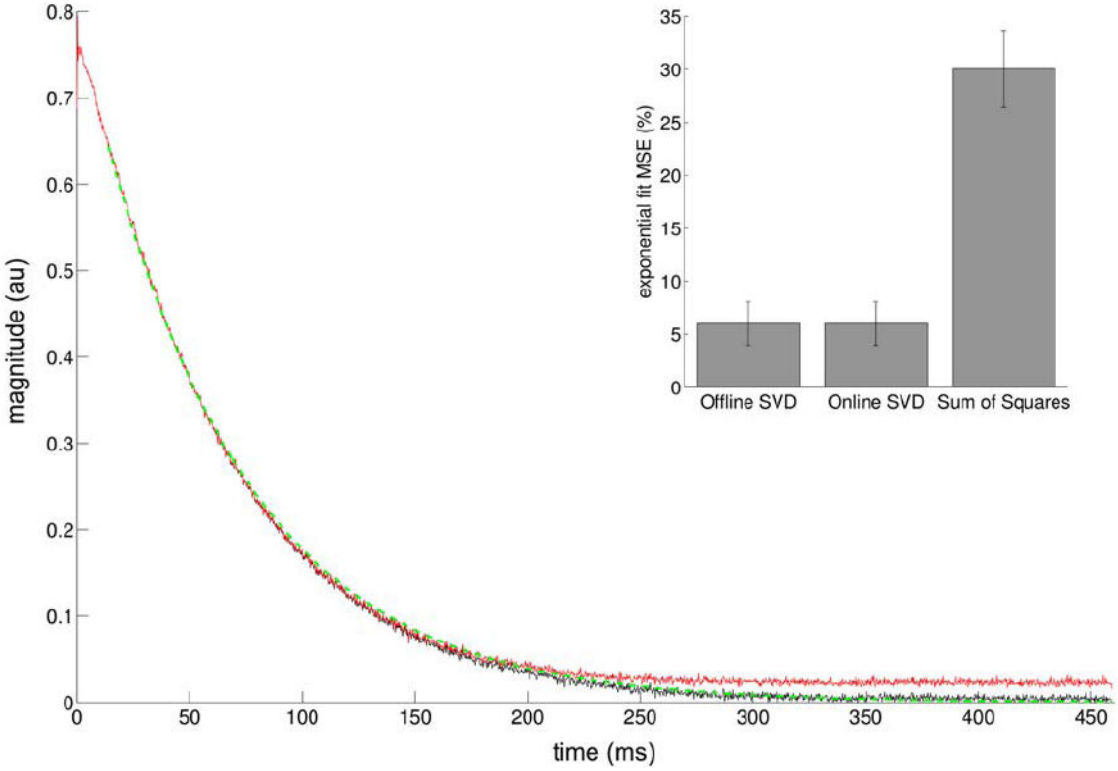

Figure 6.

Comparison of the online and offline SVD-based FID coil combination method with the widely used of Squares method. The black FID was reconstructed from 32 channels using the online SVD-based method to estimate combination weights from the first 30 measurements. The red FID was reconstructed using SoS. The green dashed line is the best fitting exponential to the SoS reconstruction (red FID). The bias introduces by SoS in low SNR conditions is apparent in the tail of the FID. The inset shows the average MSE of the exponential fit to the MVFS FIDs over subject using the offline SVD-based combine, online SVD-based combine, and Sum of Squares combine. The bias in the FID tail with SoS causes its fit MSE to be significantly higher than either the offline or online SVD-based method (*t*-test: t_3=4.3; p=0.024).

NIH-PA Author Manuscript

NIH-PA Author Manuscript

NIH-PA Author Manuscript

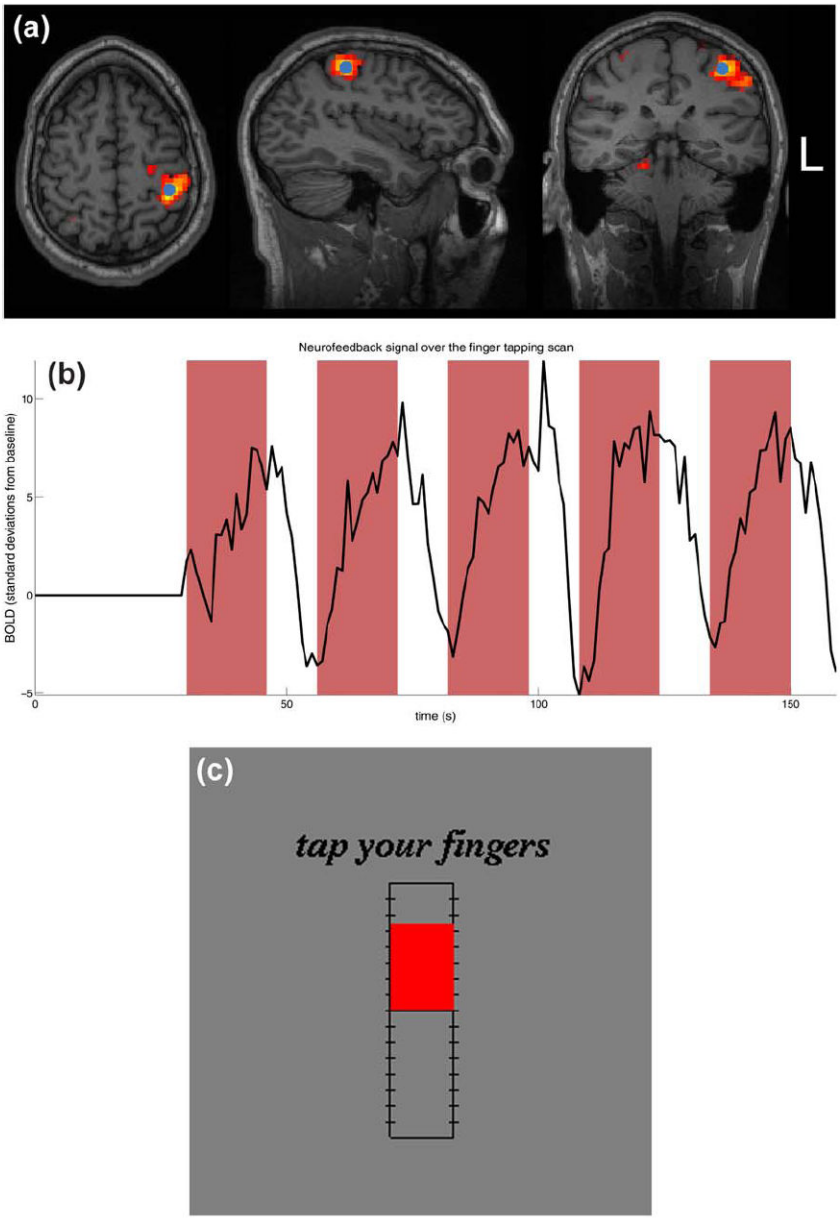

Figure 7.

(a) ROI placement, **(b)** feedback signal over the run, and **(c)** neurofeedback stimulus for the MVFS demonstration.